32nd Annual International Conference of the IEEE EMBS
Buenos Aires, Argentina, August 31 - September 4, 2010

# Exploring high-frequency oscillation as a marker of brain ischemia using S-transform

Dan Wu, *Student Member*, *IEEE*, Anastasios Bezerianos, *Senior Member*, *IEEE*, Huaijian Zhang, Xiaofeng Jia and Nitish V. Thakor, *Fellow, IEEE*

***Abstract*— Brain injury, such as hypoxic-ischemia produced in brain after cardiac arrest, is known to alter somatosensory evoked potential (SSEP) signals, thus serving a diagnostic role. This study explores the high-frequency oscillation (HFO) in SSEP recorded in a rat model of asphyxial cardiac arrest. To best characterize this complex oscillatory activity, several time-frequency representation strategies are implemented and compared. The S-transform (ST) is found to precisely localize the HFO in temporal-spectral space. More, the 'phase ST'—the inter-trial coherence (ITC) sensitively detects the phase-locked activities in HFO. Using ST and ITC, we explored the evolution of HFO during early recovery from brain injury. A discrepancy between the amplitude of HFO, which increases over time, and its phase, which stays time-invariant, is revealed here. The recovery dynamics of HFO mirrors that of N10 in terms of their amplitudes, which suggests HFO as a prelude of large-scale cortical responses. In addition, statistics shows the amplitudes of HFOs have different levels ($p$<0.05) and recovery dynamics ($p$=0.03) between the good- and bad-outcome groups. We consider the HFO to be reflective of the health of thalamocotical circuitry in brain ischemia.**

## I. Introduction

TRANSIENT somatosensory stimuli produce a series of stereotyped activation in the cerebral cortex reflected as the somatosensory evoked potentials (SSEPs). The SSEP waveform consists of a surface positive/negative complex (N10/P15 in rats) as a short-latency response, followed by a slower biphasic complex as the long-latency response. The amplitude and latency of SSEP have been extensively studied in animal models and used for clinical diagnosis and prognostication of neurological deficits [1, 2]. However, the high frequency content of SSEP attracts less attention and has not been extendedly understood.

Although historically considered a slow wave phenomenon, the SSEP exhibits high-frequency oscillation (HFO) as a series of small amplitude deflections superimposed on the short-latency complex, which becomes apparent after a high-pass filter. Two bursts of HFOs have been identified in animals [3, 4] and in humans [5, 6] within a characteristic frequency band of 400-600Hz. Early HFOs are thought to be generated by thalamocortical afferents and late HFOs are thought to be produced by cortical inhibitory interneurons [4, 6]. Thus, we believe HFO contains useful information about thalamic function and thalamocortical integrity, which enable a further investigation of the recovery mechanism from brain injury, in particular, the hypoxic-ischemic injury.

This paper studies HFO in a rat model of asphyxial cardiac arrest (CA) which induces a global brain ischemia. We will first pursue an appropriate time-frequency representation (TFR) of HFO by comparing the short-time Fourier transform, continuous wavelet transform, S-transform and inter-trial coherence. The S-transform which optimally characterizes HFO is used to present the temporal-spectral evolution of HFO during CA and early recovery. This paper discusses the interesting recovery dynamics of HFO from brain ischemia and also the statistical indications.

## II. Materials and Methods

### A. Data acquisition

The experiment was designed to assess the changes in SSEP as a result of global ischemia following cardiac arrest (CA) [7]. Sixteen male Wistar rats were subjected to either a 7min ($n$=8) or 9min ($n$=8) asphyxia. Experimental procedures were described in [8]. The epidural bipolar SSEPs were recorded with the TDT (Tucker Davis Technologies) system at a sampling rate of 6103.5Hz. Median nerve stimulation was given alternatively to the left and right forelimb through TDT microstimulator at a unilateral frequency of 0.5Hz. Signals were recorded at baseline, cardiac arrest, 1hr after CA continuously, and the next 3hrs in a 15min-on-15min-off intermittent fashion (Fig. 2(C)). Functional evaluation was performed using the Neurological Deficit Score (NDS, on a scale of 0-80) [7, 8], and a score >50 at 72hr after CA reflects a good outcome and < 50 reflects bad outcome.

SSEPs are averaged over 20 sweeps to obtain a stable waveform. A typical SSEP waveform is characterized by the N10/P15 complex with HFO overriding on the rising and falling edges of N10 (Fig. 1(A)). The signal is then filtered between 300-1000Hz with a Butterworth filter to obtain HFO.

Manuscript received April 22, 2010. This work was supported by grants RO1 HL071568 from the National Institute of Health and 09SDG1110140 from the American Heart Association.

D. Wu, A. Bezerianos, and X. Jia are with the Department of Biomedical Engineering, Johns Hopkins University School of Medicine, Baltimore, MD 21205, USA (e-mail:dwu18@jhu.edu;abezeri1@jhmi.edu; xjia1@jhmi.edu).

A. Bezerianos is with Department of Medical Physics, School of Medicine, University of Patras, Patras 26500, Greece (e-mail: bezer@upatras.gr).

X. Jia is with Department of Physical Medicine and Rehabilitation, Johns Hopkins University School of Medicine, Baltimore, MD 21205, USA (e-mail: xjia1@jhmi.edu)

H. Zhang is with Department of Biomedical Engineering, Zhejiang University, Hangzhou 310027, China (e-mail: alexwillzhj@hotmail.com)

N. V. Thakor is with the Department of Biomedical Engineering, Johns Hopkins University School of Medicine, Baltimore, MD 21205, USA (phone: 410-955-7093; fax: 410-955-1498; email: nitish@jhu.edu ).

### B. Short Time Fourier Transform (STFT)

The discrete STFT is performed as an initial try to characterize the HFO in the TF domain. In STFT, a time series is multiplied by a window function whose center slides over time to track localized spectral distribution. Mathematically, the STFT of a signal $x(n)$ is written as:

$$X_w(t,f) = \sum_{n=-\infty}^{\infty} x(n)w(n-t)e^{-j2\pi fn} \quad (1)$$

where $w(n)$ is a window function, commonly a Hanning window centered at zero, and $X_w(t,f)$ is a complex function indicating the phase and magnitude of the signal over time and frequency.

### C. Continuous Wavelet Transform (CWT)

The CWT is also examined in this paper to provide a multi-resolution TFR by time-scaling and time-shifting a prototype function $\psi(t)$, so called the mother wavelet. The CWT decomposes a signal into a collection of shifted and scaled versions of the mother wavelet $\psi(t)$ through

$$W(a,b) = \frac{1}{\sqrt{a}}\int_{-\infty}^{\infty} x(t)\psi^*(\frac{t-b}{a})dt \quad (2)$$

where $a$ is the scaling factor that relates (inversely) to the radian frequency and $b$ is the shifting factor that determines the time increment. * denotes the complex conjugate operation when $\psi(t)$ is a complex function. The Morlet wavelet is chosen as the base function because of its similarity to HFO in shape.

### D. S-transform (ST)

The ST is a complex transformation that outputs a localized estimation of the time-varying energy as well as the phase of the analyzed signal, proposed by R. G. Stochwell et al. in 1996 [9]. It is defined as:

$$S(\tau,f) = \int_{-\infty}^{\infty} x(t)\frac{|f|}{\sqrt{2\pi}}e^{\frac{(\tau-t)^2 f^2}{2}}e^{-j2\pi ft}dt \quad (3)$$

The ST can be derived from STFT by applying a frequency-dependent Gaussian window of $g(t) = \frac{1}{\sigma\sqrt{2\pi}}e^{-\frac{t^2}{2\sigma^2}}$, where $\sigma=1/f$. It can also be seen as a derivation from CWT by $S(\tau,f) = \sqrt{\frac{f}{2\pi}}e^{-j2\pi f\tau}W(\tau,f)$, where the mother wavelet is defined as $\psi(t,f) = e^{-\frac{t^2f^2}{2}}e^{-j2\pi ft}$.

### E. Inter-trial Coherence (ITC)

The ITC [10] is used for detection of the degree of phase-locking between trials based on the ST.

$$ITC(t,f) = \left\| \frac{1}{N}\sum_{i=1}^{N} e^{j\phi_i(t,f)} \right\| \quad (4)$$

where $\emptyset(t,f)$ is the phase-spectrum of Eq. (3) which can be writen as $S(\tau,f) = A(\tau,f)e^{-j\emptyset(\tau,f)}$, and $N$ is the total number of trials. $ITC(t,f)$ is within the range [0, 1] with 1 stands for strictly phase-locked activity and 0 for purely non-phase-locked acitvity. We derived the ITC on a base of 20 raw sweeps of SSEPs.

## III. Results and Discussion

### A. Time-frequency Representation of HFO

The TFR approaches discussed above have been applied on HFO and resultant TF spectrograms ($\|X_w(t,f)\|$, $\|W(t,f)\|$, $\|S(t,f)\|$, $\|ITC(t,f)\|$) are compared in Fig. 1(B). All TFR gave approximately the same results with a peak at 10ms for low-frequency SSEP, and a second peak around 400Hz slightly before 10ms for HFO. However, the features of different TFRs are distinct: the CWT exhibits the fine details about low-frequency SSEP, but fails to localize the very transient type of signal; the ST appears to be the best representation of fast oscillatory pattern of event, which precisely captures the location of HFO in the TF domain; whereas the STFT is poor in both time and frequency resolution, due to the very short duration of signal. The performance of ST on HFO is in agreement with the simulation study by Stockwell [9] about the superiority of ST on high frequency bursts.

As described in the methods section, the ST is an extension of STFT and CWT, which possesses some desirable properties that are absent in STFT or CWT. On one hand, the ST is a special case of STFT with a moving and scalable Gaussian window, incorporating $\sigma=1/f$ as the width of the window (3). In such a way, the ST provides a frequency-dependent multi-resolution STFT as well as higher time resolution owning to the use of Gaussian kernel. On the other hand, the ST can be defined as a CWT with a specific mother wavelet multiplied by a phase factor $e^{-j2\pi ft}$ which corrects the phase information to be always referenced to time $t=0$. Therefore, the ST uniquely combines frequency-dependent resolution with absolutely referenced local phase information [11], thus exhibits superiorities for the representation of HFO.

The phase information from ST, the ITC, is directly related to the concept of phase-locking, which is essentially a measurement of consistency across stimulus-locked trial activities at each frequency and latency window. Note that in the definition of ITC (4), the complex spectrum is first normalized to unit length (phase is extracted) and then averaged. This makes the ITC more sensitive to phase disturbances, even very low-amplitude signals can be detected provided that they are highly phase-locked [12]. As we can see from the ITC of the unfiltered SSEP signal (Fig. 1(A)), marked phase-locking phenomenon exists in both high- frequency and low-frequency bands, regardless of the small amplitude of HFO compared to that of the N10/P15 complex. The strong phase-locking in HFO is believed to reset the ongoing EEG activity in response to the stimuli [13].

Considering the benefits and drawbacks of various TF transformations, we consider the ST as the most useful TFR for the purpose of detecting HFO. In this study, HFO is detected by finding a peak in the ST spectrum, as detection of fast oscillations in time-domain is more difficult. Accordingly, $\|S(t,f)\|_{max}$ is used as a measurement of amplitude-related activation, and $\|ITC(t,f)\|_{max}$ as a measurement of phase-related coherence.

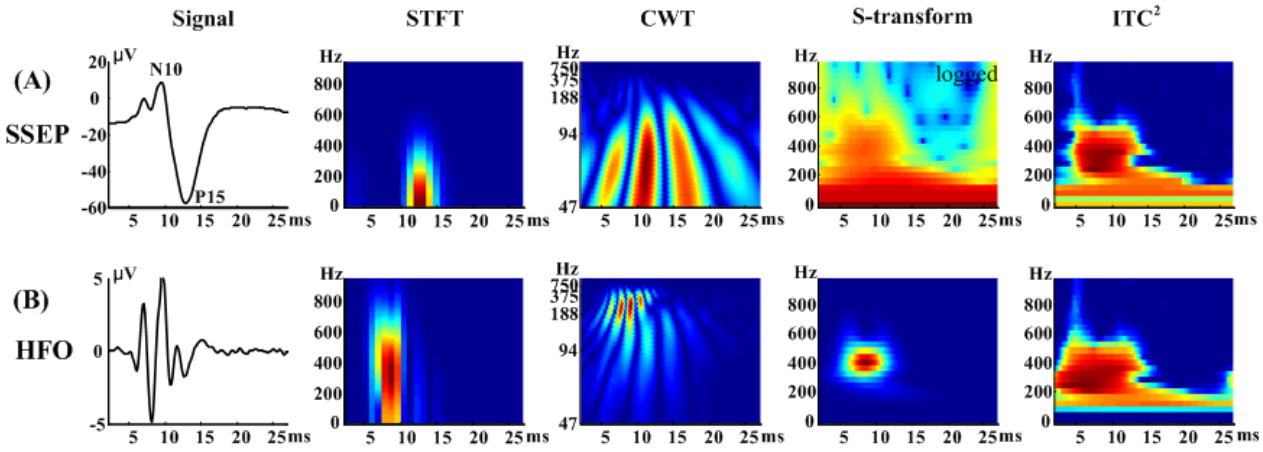


Fig. 1. Short Time Fourier Transformation (STFT), Continuous Wavelet Transform (CWT), S-transformaton, Inter-trial Coherence (ITC) on (A) unfiltered SSEP and (B) HFO. The signal is taken from a 20-sweep averaged SSEP from a baseline recording. HFO is high-pass filtered from SSEP within 300-1000Hz. Note that the $||S(t,f)||$ of the SSEP signal is log-transformed in order to adjust the heavily left-skewed distribution of values, and the $||ITC(t,f)||$ of both HFO and SSEP are squared because of their right-skewed distribution.

### *B. Evolution of HFO in CA model*

A typical HFO in this study consists of a 'spike' on the rising edge of N10 and a smaller 'spike' on the falling edge of N10, followed by short residual ripples, which form a spindle-like oscillation. In all of the 16 experimental rats, the HFO is found to disappear during cardiac arrest, and recur after resuscitation. The recurring time varied between 20-50min along the experiment timeline. The amplitude of HFO was extremely low at first, which gradually grew as the rats recovered (Fig. 2(A)), but never reached the baseline level even at the end of recording (4hr after ROSC). The evolution of HFO can be better visualized in the TF domain by ST, where the temporal-spectral peak of HFO became scattered at the onset of CA and then returned with the same pattern but increasing amplitude (Fig. 2(B)).

The recovery dynamics of HFO is surprisingly similar to that of N10 in terms of their amplitudes (Fig. 3). The trend of N10 amplitude is essentially a duplicate of that of the HFO, except for the different intercepts. The correlation coefficient between these two trends is above 0.9 for 13 out of the 16 rats, meaning that the HFO and N10 dynamics are basically following the same process. Such similarity is in line with the general belief that the HFO originates from thalamocortical axonal activity that activates N10, so that stronger activation evokes larger response and vice-versa. On the other hand, the normalized HFO amplitude is always above that of the N10, and also the HFO tends to recur earlier than the N10. The seemingly better and earlier recovery of HFO over N10 agrees with other studies that the cortex is more vulnerable to global brain ischemia compared to the thalamus [14].

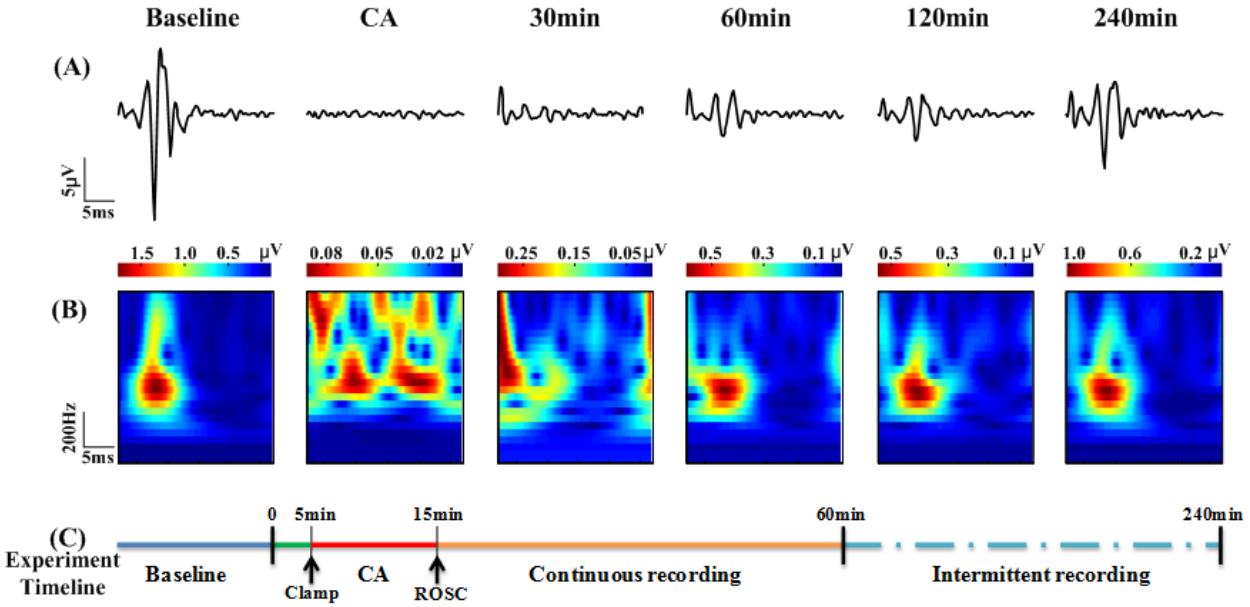


Fig. 2. Evolution of HFO at baseline, cardiac arrest and recovery periods at 30min, 60min, 120min, and 240min. Panel (A) shows the evolution of a typical HFO waveform. Panel (B) shows the corresponding S-transformations of the signals in (A). The color map of each TF spectrum shows the relative strength to its maximum, with the absolute values indicated in the color bar. Notice that the recurred HFO has a similar temporal-spectral peak as the baseline but much smaller amplitude. Panel (C) illustrates the experiment timeline for all the experiments in this study.

In contrast with the severely hampered amplitude, the TF pattern of HFO is always consistent with the baseline. Once the HFO recurred, it kept strictly phase-locked to the stimulus with no delay, unlike the delayed N10 peak at the beginning of recovery (Fig. 3). The strength of phase-locking in HFO is quantified using ITC, and compared with the latency of N10. Assuming that the HFO is a reflection of spike activity from the thalamocortical input axons, the time-invariant phase-locking phenomenon would indicate that the thalamus activates the cortex at a fixed tone, while the cortical response may be delayed due to weak thalamocortical coupling.

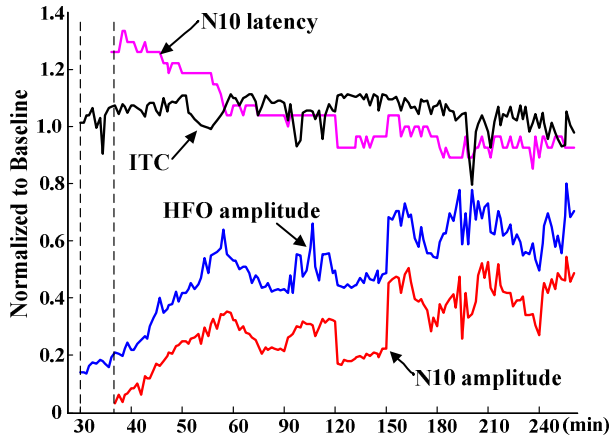


Fig. 3. Trends of the inter-trial coherence (ITC) of HFO, amplitude of HFO, and amplitude and latency of N10 during recovery from CA. The HFO amplitude is obtained using $\|S(t,f)\|_{max}$ and coherence is measured by $\|ITC(t,f)\|_{max}$ (values normalized to baseline). Notice that the HFO recurs at 30min, whereas the N10 recurs 7min later than the HFO.

### C. *Statistic dynamics*

In order to assess the behavior of HFO over all subjects, we grouped them into the good-outcome (72hr NDS>50, G1) and bad-outcome (72hr NDS<50, G2) groups. Shown in Fig. 4, the HFO amplitude is significantly higher in G1 during 30-180min after CA, but gets saturated towards the end and no long differentiates between groups, pointing to the unique prognostic value of HFO in early recovery stage. Repeated measures ANOVA shows the group difference plays an important role in the regression of HFO amplitude over time ($p$=0.03), indicating the different recovery dynamics between the two outcome groups. The rats in G1 tend to recover faster and stabilize earlier than the ones in G2.

## IV. Conclusion

The paper establishes the ST as a useful TFR of HFO, with the help of which we investigated the change of HFO in a CA-induced global brain ischemia model. Results show that HFO is substantially depressed after CA, but it maintains a strong phase-locking to the stimulus. The amplitude of HFO is found to be tightly correlated with that of the N10, and is associated with long-term neurological outcome.


## Acknowledgment

The authors would like to thank Dr. Young-Seok Choi for discussions on methods, and Jai Madhok for editions.


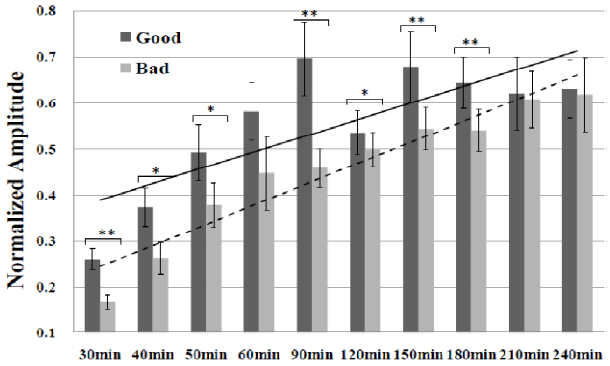


Fig. 4. HFO amplitudes for the good-outcome (72hr NDS>50) and bad-outcome (72hr NDS<50) groups at different stages after CA (normalized to baseline). The solid and dashed trendlines are linearly-fitted regression lines for the good- and bad-outcome groups, respectively. (*$p$<0.05, **$p$<0.01; one-tailed Student's $t$-test under assumption of unequal variances)

## References


[1] S. J. Jacinto, M. Gieron-Korthals, and J. A. Ferreira, "Predicting outcome in hypoxic-ischemic brain injury," *Pediatr Clin North Am,* vol. 48, pp. 647-60, Jun 2001.

[2] E. G. Zandbergen, A. Hijdra, J. H. Koelman, A. A. Hart, P. E. Vos, M. M. Verbeek, and R. J. de Haan, "Prediction of poor outcome within the first 3 days of postanoxic coma," *Neurology,* vol. 66, pp. 62-8, Jan 10 2006.

[3] H. Ikeda, L. Leyba, A. Bartolo, Y. Wang, and Y. C. Okada, "Synchronized spikes of thalamocortical axonal terminals and cortical neurons are detectable outside the pig brain with MEG," *J Neurophysiol,* vol. 87, pp. 626-30, Jan 2002.

[4] S. N. Baker, G. Curio, and R. N. Lemon, "EEG oscillations at 600 Hz are macroscopic markers for cortical spike bursts," *J Physiol,* vol. 550, pp. 529-34, Jul 15 2003.

[5] R. Gobbele, H. Buchner, and G. Curio, "High-frequency (600 Hz) SEP activities originating in the subcortical and cortical human somatosensory system," *Electroencephalogr Clin Neurophysiol,* vol. 108, pp. 182-9, Mar 1998.

[6] I. Hashimoto, T. Mashiko, and T. Imada, "Somatic evoked high-frequency magnetic oscillations reflect activity of inhibitory interneurons in the human somatosensory cortex," *Electroencephalogr Clin Neurophysiol,* vol. 100, pp. 189-203, May 1996.

[7] X. Jia, M. A. Koenig, H. C. Shin, G. Zhen, C. A. Pardo, D. F. Hanley, N. V. Thakor, and R. G. Geocadin, "Improving neurological outcomes post-cardiac arrest in a rat model: immediate hypothermia and quantitative EEG monitoring," *Resuscitation,* vol. 76, pp. 431-42, Mar 2008.

[8] W. Xiong, M. A. Koenig, J. Madhok, X. Jia, H. A. Puttgen, N. V. Thakor, and R. G. Geocadin, "Evolution of Somatosensory Evoked Potentials after Cardiac Arrest Induced Hypoxic-Ischemic Injury," *Resuscitation,* vol. in press, 2010.

[9] R. G. Stockwell, L. Mansinha, and R. P. Lowe, "Localization of the complex spectrum: the S transform.," *IEEE Trans Signal Process,* vol. 44, pp. 998-1001, 1996.

[10] S. Makeig, M. Westerfield, T. P. Jung, S. Enghoff, J. Townsend, E. Courchesne, and T. J. Sejnowski, "Dynamic brain sources of visual evoked responses," *Science,* vol. 295, pp. 690-4, Jan 25 2002.

[11] R. G. Stockwell, "Why use the S-transform?," *AMS Pseudo-differential operators: partial differential equations and time-frequency analysis,* vol. 52, pp. 279-309, 2007.

[12] C. Tallon-Baudry, O. Bertrand, C. Delpuech, and J. Pernier, "Stimulus specificity of phase-locked and non-phase-locked 40 Hz visual responses in human," *J Neurosci,* vol. 16, pp. 4240-9, Jul 1 1996.

[13] M. Valencia, M. Alegre, J. Iriarte, and J. Artieda, "High frequency oscillations in the somatosensory evoked potentials (SSEP's) are mainly due to phase-resetting phenomena," *J Neurosci Methods,* vol. 154, pp. 142-8, Jun 30 2006.

[14] R. Canese, F. Podo, S. Fortuna, P. Lorenzini, and H. Michalek, "Transient global brain ischemia in the rat: spatial distribution, extension, and evolution of lesions evaluated by magnetic resonance imaging," *MAGMA,* vol. 5, pp. 139-49, Jun 1997.